



Evaluation of the System-Aggregated Potentials of Inertial Support Capabilities from Wind Turbines

Downloaded from: <https://research.chalmers.se>, 2026-04-04 15:40 UTC

Citation for the original published paper (version of record):

Imgart, P., Chen, P. (2019). Evaluation of the System-Aggregated Potentials of Inertial Support Capabilities from Wind

Turbines. Proceedings of 2019 IEEE PES Innovative Smart Grid Technologies Europe, ISGT-Europe 2019. <http://dx.doi.org/10.1109/ISGTEurope.2019.8905488>

N.B. When citing this work, cite the original published paper.

© 2019 IEEE. Personal use of this material is permitted. Permission from IEEE must be obtained for all other uses, in any current or future media, including reprinting/republishing this material for advertising or promotional purposes, or reuse of any copyrighted component of this work in other works.

Evaluation of the System-Aggregated Potentials of Inertial Support Capabilities from Wind Turbines

Paul Imgart

Division of Electric Power Engineering
Chalmers University of Technology
Göteborg, Sweden
Email: paul.imgart@chalmers.se

Peiyuan Chen

Division of Electric Power Engineering
Chalmers University of Technology
Göteborg, Sweden
Email: peiyuan@chalmers.se

Abstract—The increasing shift from synchronous towards converter interfaced generation and consumption changes the mechanical inertia in power systems. Thus it is of great importance for system operators to estimate the potentials of inertial support from the wind turbines connected to their systems.

This paper utilizes meteorological re-analysis data in conjunction with a wind turbine database in a novel way to estimate the inertial support capabilities of all wind turbines in Sweden. Using the wind speed profile across the country for the years 2010 - 2015, a linear relation between energy production and inertial support capability of 1.3 Ws/W is shown for the investigated inertial support approach. Furthermore, the results show that the 7.48 GW installed converter-interfaced wind turbines in Sweden can provide, on average, kinetic energy of 2.72 GWs and inertial support power of 0.27 GW, which is equivalent to 19.3 % of the Nordic system dimensioning fault.

Index Terms—Distributed power generation, inertia, load-frequency control, meteorological factors, primary frequency control, wind energy integration, wind turbine modeling

I. INTRODUCTION

In 2017, the installed wind power generation capacity in the EU-28 countries reached a share of 18 % of the total generation capacity [1]. Together with a shift in wind turbine technology towards variable speed wind turbines and a simultaneous increase in solar power, this leads to a significant increase of inverter connected generation. In consequence the system inertia decreases due to the replacement of synchronous generation, which challenges the frequency stability of the power system. In response to this, using the kinetic energy of wind turbine for inertial support has been a focus of recent research.

In [2] an overview of the importance of inertia and possible effects of an increase in converter connected generation is given. This is supplemented by [3] and [4] with the findings about the impact of different wind turbine types on system frequency control. Existing literature has focused on the controller design of wind turbines to provide inertial support to the grid (e.g. [5]–[8]). The studies about the aggregated effects of wind turbine inertial support share the problem that the operating states of the turbines in the system are unknown. To solve this, some assume an uniform operating state for all wind turbines (e.g. [9], [10]). However, as shown by [11] and [12], the available kinetic energy from wind turbines varies greatly with the operating point, which challenges this assumption. Others such as [4] have chosen a curve fitting

approach to deduct a relation between a known quantity (e.g. wind power generation) and wind turbine kinetic energy or available inertial support respectively. This deduction is based on a limited sample, e.g. historical data from test wind farms. Due to the small data base, it remains unknown if the inferred relation holds for the complete system with spatially dispersed wind turbines. Furthermore, no information is retained about the variability and the extrema. A different approach is to use probabilistic methods to derive the desired relation from historical data, e.g. in [13] and [14]. This strategy also does not include information about extreme conditions, which are of special interest for power system stability analysis. Furthermore a constant, unchanged spatial distribution of wind turbines is necessary for the derived wind speed distribution to remain valid. The validity of the undertaken assumptions and simplifications remains unproved.

The main purpose of this paper is to calculate the total kinetic energy available from all variable-speed wind turbines to provide inertial support to the power grid in case of frequency disturbances. Its main contribution is the numerical quantification of the relation between the system wind power generation and the corresponding inertial support capability. It exhibits a linear behavior at system level if each wind turbine contributes with a fixed inertial power (e.g. 0.1 p.u.), but becomes highly nonlinear when the inertial power increases. This is achieved by an innovative usage of historical timeseries of meteorological re-analysis wind speed data in conjunction with a wind turbine database to determine the operating states of the turbines throughout the system. Employing static and dynamic wind turbine models and aggregating their results for the entire system, the kinetic energy available to the system is computed by a link of system of models following the physical causalities instead of the deduction based on assumptions or correlation present in literature on this topic. This methodology is an additional contribution of this paper.

II. WIND ENERGY CONVERSION MODEL

In this paper, realistic operating conditions are simulated for the wind energy conversion (WEC) units in a power system to evaluate the inertial support potentials from wind turbines. This is accomplished by using historical spatial wind speed distributions from meteorological re-analysis data and

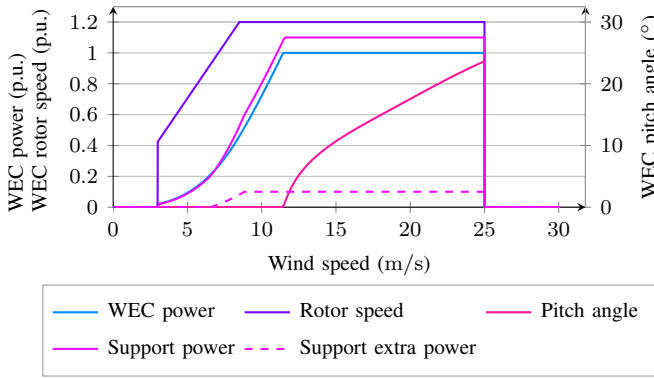


Fig. 1. WEC power and rotor speed in p.u. over wind speed in m/s as simulated by the steady-state wind turbine model. Also contains the inertial support power for the 0.1 p.u. inertial support approach.

combining them with a database of the Swedish wind turbines and a steady-state WEC model.

In a first step the wind speed at hub height is estimated for all wind turbines in the database for each hour during the years 2010-2015 by interpolation of MERRA-2 meteorological data from [15]. After corrections to the wind turbine database, those wind speeds are used to estimate the operating points of each wind turbine for each point in time with the help of a steady-state wind turbine model. Details of the model exceeding the description in this section can be found in [16].

The steady-state wind turbine model is based on [17] and represents the relevant parts of a 3.6 MW doubly-fed induction generator (DFIG) turbine. The drive train is modelled as a lumped, single mass, and the turbines power conversion from mechanical to electrical power is assumed to be lossless. The dynamics of the electrical systems and corresponding control are assumed to be much faster than the rotor speed dynamics and are therefore not modelled in detail.

The wind turbine power generation is characterized as

$$P_{\text{WEC, mec, pu}} = \frac{1}{2} \rho_{\text{air}} \cdot A_r \cdot v^3 \cdot C_p(\lambda, \beta). \quad (1)$$

$P_{\text{WEC, mec, pu}}$ denotes the wind turbines mechanical power in p.u., ρ_{air} is the air density in kg/m^3 , $A_r = A \cdot P_n^{-1}$ is the ratio between the turbines rotor area and its rated power in m^2/W , v is the wind speed at hub height in m/s and C_p is the dimensionless power coefficient, which is calculated by the mathematical representation given in [17], depending on the pitch angle β and the tip speed ratio λ determined by

$$\lambda = K_b \cdot \frac{\omega_{\text{pu}}}{v} \quad \text{with } K_b = R \cdot \omega_{\text{base}}, \quad (2)$$

where K_b denotes the turbine's rated tip speed in m/s, i.e. the product of the rotor radius R and the base rotor speed ω_{base} . The parameters used in this work are given in the appendix.

The rotational friction and generator losses are accounted for by adjustment of the wind speeds through comparison of the documented annual energy production with the calculated one, so the mechanical power is equal to the electrical power:

$$P_{\text{WEC, el, pu}} = P_{\text{WEC, mec, pu}}. \quad (3)$$

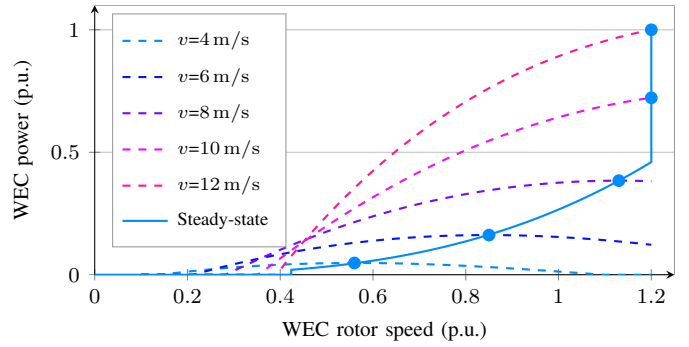


Fig. 2. WEC power over rotor speed for different wind speeds for constant intended steady-state operation pitch angle, including curve of intended steady-state operation.

The wind turbine power as given in (1) is not solely dependent on the wind speed, but can also be influenced by the choice of rotor speed and pitch angle. The resulting wind turbine control scheme can be divided into three wind speed ranges.

- 1) *Low wind speed*: The low wind speed range starts with cut-in wind speed and ends when the turbine has reached its maximum rotor speed. In this wind speed range, the wind turbine operates in the maximum power point (MPP) by controlling the rotor speed to match the optimal tip speed ratio, resulting in the maximum power coefficient. The rotor speed increases linearly with the wind speed, while the power increases cubically.
- 2) *Medium wind speed*: The medium wind speed range is the wind speed range where the wind turbine already operates at maximum rotor speed but not maximum power. The constant rotor speed results in a decreasing tip speed ratio and aerodynamic efficiency, which is reflected by a falling power coefficient C_p . An increased wind speed still results in an increased WEC power.
- 3) *High wind speed*: The high wind speed range is between the wind speed where the turbine reaches maximum power and the cut-off wind speed. In this range the turbine operates at the maximum rotor speed and power. To limit the power, the power coefficient is reduced by changing the pitch angle of the turbine accordingly.

This turbine behaviour is simulated for wind speed steps of 0.01 m/s and the resulting rotor speed, pitch angle and WEC power are saved in a lookup table. The computed power curve is given in Fig. 1 including rotor speed and pitch angle. The three wind speed ranges can be determined easily in the figure.

While this curve is valid for intended steady-state operation, the model also allows for the calculation of other operating points by recalculating the C_p -value according to the given tip speed ratio λ . Fig. 2 shows the WEC power in dependence of rotor speed for different wind speeds, which highlights the decrease in aerodynamic efficiency with higher distance from the steady-state operation point (with exception of few cases at very high wind speeds not displayed in the figure). This is relevant for the dynamic behaviour of the turbines during

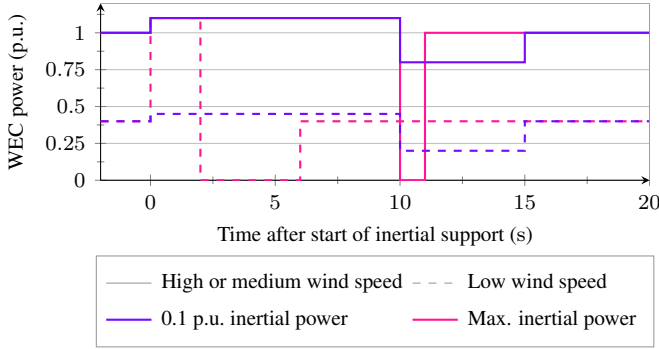


Fig. 3. Example time series of inertial support for different wind speed ranges.

inertial response, where their rotor speeds vary from steady-state operation.

The rotor speed and hourly average power estimated by the steady-state wind turbine model is ultimately assigned to all WEC in the database for every hour in the simulated time span according to the interpolated wind speed at hub height, scaled to their respective rated power. The results can then be compared to the aggregated time series from [18]. The deviation in annual energy production amounts to an overproduction of 6.39% compared to the reference. The most important reasons for this deviation are the limited spatial and temporal resolution of wind speed data, the application of a single power curve to all wind turbines, the neglect of site-specific influences such as terrain structure and wake effects as well as the simplified representation of the losses. While these inaccuracies have a non-neglectable influence on the outcome of subsequent computations, it is assumed that their influence on the trends and relations in the final results is limited.

III. SINGLE TURBINE INERTIAL RESPONSE

To simulate the inertial response of a single wind turbine, a dynamic wind turbine model is introduced and subjected to a variation in electrical power at a given, constant wind speed. Due to the power imbalance, kinetic energy is fed into the grid and the turbines rotor speed changes. This deviation from intended steady-state operation results in a change in aerodynamic efficiency, which is an important factor to be considered in the simulation of wind turbine inertial response.

A. Operating Limits

The main phenomena that limit the rotor speed deviation from synchronous speed are rotor current and voltage limits in DFIG machines and the reduced aerodynamic lift of the turbine rotor. A second important operating limit is the short term overloading limit of generator and converter. To respect these limits, the minimum rotor speed is set to 0.1 p.u. [17], the minimum mechanical power to 0.025 p.u. and the short term maximum electrical power to 1.1 p.u. [8]. For a more realistic simulation of the operating limits for wind turbine inertial response, it is necessary to conduct field studies testing and improving the accuracy of the suggested operating limits.

B. Control Approaches

There exist various control strategies to make the kinetic energy of wind turbines available for inertial response, which can be divided into three different categories [19]: Frequency independent, frequency deviation dependent, and finally frequency derivative and deviation dependent. Here a frequency independent approach is chosen, because it allows to evaluate the total available WEC kinetic energy from the planning perspective and provides an upper limit for real-time operation.

Obviously, this choice introduces many degrees of freedom in the design of the pre-determined inertial support response. In this work, the length of the support phase has been devised to 10s. The additional power from inertial support rises linearly with the turbine power from 0 p.u. to 0.1 p.u. between a steady-state power of 0.2 p.u. and 0.5 p.u., from where it stays constant at 0.1 p.u.. This is illustrated by the dashed line in Fig. 1. During the recovery phase, the electric power is reduced by 0.2 p.u. from the steady-state power. This approach resembles the specifications of the transmission system operator Hydro-Quebec as given in [20] and the actual implementation in a WEC as documented in [17] and is also supported by the average time to frequency nadir during disturbance, which should lie inside the chosen support time and is specified as 8.7s in [21]. A second approach is simulated to provide the maximum inertial power from a wind turbine until any of the operating limits or the maximum support time of 10s is reached. This approach is to illustrate the maximum inertial power extractable from a wind turbine. Fig. 3 contains example time series of WEC power during support and recovery phase for low, medium and high wind speeds using the 0.1 p.u. inertial power support and the maximum inertial power support.

C. Dynamic Wind Turbine Model

The rotor dynamic model is simulated according to

$$2H \cdot \omega_{pu} \frac{d\omega_{pu}}{dt} = P_{mech,pu} - P_{el,pu} \quad (4)$$

with the turbine's inertia constant H in s. In each simulation step, the electrical power output $P_{el,pu,k}$ is updated according to the specified inertial response and the mechanical power $P_{mech,pu,k}$ is recalculated with the help of (1) assuming a constant pitch angle and wind speed. Furthermore it is checked if a turbine has tripped due to reaching operating limits.

After the end of the support phase at 10s, the electrical power output is changed to the recovery power and the simulation is continued until the turbine meets its initial rotor speed again. In the case a turbine is tripped, recovery commences immediately and electrical power output is set to zero. While during the support phase the turbines pitch angle is only changed if necessary to limit the power output to its maximum of 1.1 p.u., it is optimised for minimum recovery time during the recovery period.

D. Results of Single Turbine Inertial Response Simulation

A first result of the simulations is that the turbines do not reach the operating limits at any wind speed for the

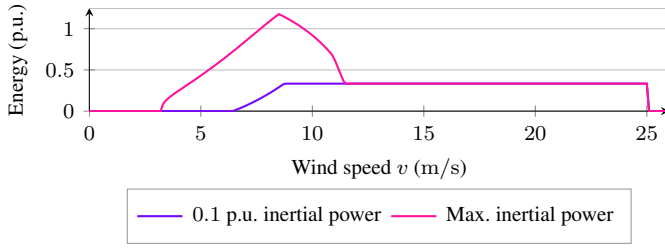


Fig. 4. Inertial support energies with respect to wind speeds. 1 p.u. corresponds to the kinetic energy stored in the rotating mass of the wind turbine when rotating at the rated rotor speed.

0.1 p.u. inertial power support, but only during the maximum inertial power approach. To be able to further quantify the inertial support capabilities and to analyze the influence of the operation points it is necessary to introduce different analytical measures. Here only the inertial support energy is discussed, but [16] contains further characteristics and analyses about the impact of different turbine parameters.

The inertial support energy is the additional energy fed to the grid during the inertial support phase. The energy base is calculated as the product of the turbine rated power and inertia constant, where 1 p.u. corresponds to the turbine's kinetic energy at rated rotor speed. Fig. 4 shows the inertial support energy in per unit for different wind speeds.

For the 0.1 p.u. inertial power support, the support energy (over a period of 10 s) curve follows the support power curve shown in Fig. 1. Beginning with a wind speed of 6.5 m/s, where the steady-state power reaches the lower limit for inertial support of 0.2 p.u., the support energy increases until reaching its maximum of 0.33 p.u. at 8.8 m/s corresponding to a steady-state power of 0.5 p.u., from where on the support energy stays constant. The maximum inertial power support simulation reaches its peak in support energy at 8.5 m/s, i.e. the wind speed where the turbine first reaches maximum rotor speed. This is because at this point of operation the turbine already has maximum kinetic energy while the spare capacity between the stationary power output and the power output during inertial response (i.e. the turbine maximum electric power output) is still big, which allows for a fast injection of energy into the grid without losing too much energy due to the reduced efficiency. Beyond this wind speed, the support energy is reduced again throughout the medium wind range, because the aerodynamic losses due to the rotor speed variation are increasing (see the steeper curves for higher wind speeds in Fig. 2) and the smaller difference between the maximum power output and the stationary power demands a longer support period, while the available kinetic energy does not increase further. From 11.45 m/s on, i.e. at wind speeds where the steady-state power is 1 p.u., the support energy remains constant and equal to the 0.1 p.u. inertial power support approach due to the turbines maximum power output limit of 1.1 p.u. The support energy of the maximum inertial power support simulation peaks at a value of 1.18 p.u., which is 82% of the maximum kinetic energy, while the 0.1 p.u.

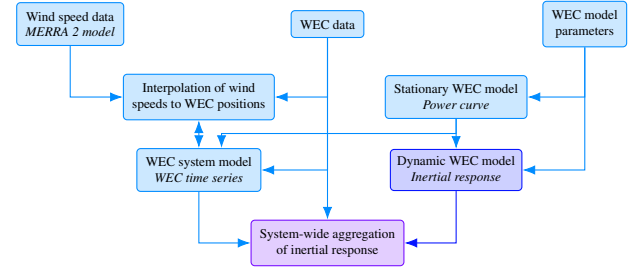


Fig. 5. Structure of the simulation model.

inertial power support approach reaches a share of 23%.

It can be concluded, that for the investigated turbine model the 0.1 p.u. inertial power support shows few negative effects for operation around $v_{\omega_{max}}$ and at wind speeds above 12 m/s, while in other operational ranges the costs in form of losses and the risks of turbine instability are greater due to a lower minimum rotor speed.

IV. AGGREGATED WIND TURBINES INERTIAL RESPONSE

To allow conclusions about the system resilience of wind turbines providing inertial support, it is necessary to transfer the individual turbines inertial response to all the turbines in the system according to their operational state. This is achieved by estimating the steady-state operating point of all wind turbines through the combination of the wind speed and the WEC data. Then the inertial response for all turbines can be aggregated according to their current operating state, which is done for each hour in the years 2010 to 2015. Fig. 5 shows the scheme for obtaining the system-aggregated inertial support. The index of highest interest is the aggregation of the inertial support energy, which is displayed in respect to the wind power production along the wind turbine kinetic energy in Fig. 6. The solid line depicts the mean and the colored area includes all values between 5th and 95th percentile. The figure shows the results for the wind turbine scenario A1 [18] (i.e. an installed capacity of 7.48 GW) and wind speed data from 2010 to 2015. Further results and analysis for both single turbine and aggregated inertial support can be found in [16].

The total kinetic energy curve (top blue curve) reaches a maximum approx. 31.9 GW s at the maximum hourly production of 7.3 GW h/h. The steeper increase for lower wind scenarios can be explained referring to Fig. 1, which shows that turbines reach their maximum rotor speed and kinetic energy at relatively low wind speeds. For higher wind scenarios many turbines consequently already operate at their maximum rotor speed and do not gain additional kinetic energy.

In contrast, the support energy of the 0.1 p.u. inertial power support approach increases rather linearly with small spread with the increase of system energy production. For the maximum inertial power support simulation the behaviour of the support energy is resembling the total kinetic energy in the lower third of the hourly energy production spectrum, but reaches its maximum at approximately 3.5 GW h/h. At higher production, the support energy declines again until

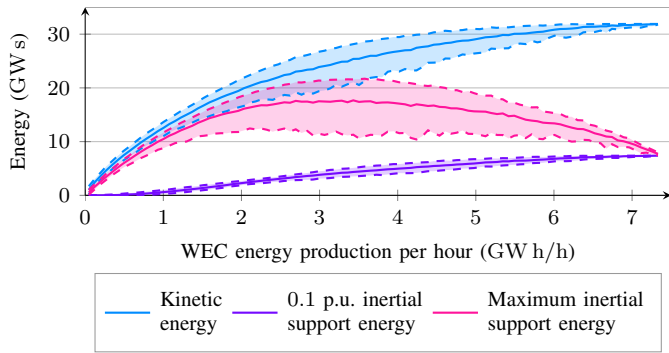


Fig. 6. Aggregated inertial support energies over the system-wide WEC hourly energy production.

it nearly meets the 0.1 p.u. inertial power support approach at the maximum production with a value of 7.8 GW s. This curve also has its greatest variance at medium production and spreads stronger than the other curves. The decline at higher production scenarios can be easily explained with Fig. 4. At higher wind speeds, the short term converter limit of 1.1 p.u. reduces the extra support energy available for the grid for higher productions. This indicates that for the maximum inertial power approach the maximum inertial support power and energy do not occur at the largest wind power production.

V. CONCLUSION

This paper has dealt with the aggregated inertial response of wind turbines by employing an innovative combination of meteorological and wind turbine databases with wind turbine models, representing the most relevant physical processes in their spatial distribution. It has shown that for the 0.1 p.u. inertial response approach a linear correlation between the aggregated WEC energy production and the available inertial support energy can be assumed. The Pearson correlation coefficient for this relation is 0.975 with a gradient of 1.3 W s/W. For other inertial support approaches, e.g. maximum inertial power, no linearity should be assumed.

Due to the great variability of wind turbine energy production between 0.01 GW h/h and 7.37 GW h/h, the inertial support energy of the 0.1 p.u. inertial response approach ranges between 0 GW s and 7.38 GW s and the inertial support power between 0 GW and 0.74 GW. The averages are 2.72 GW s and 0.27 GW, respectively. The maximum inertial support power of the Swedish wind turbines in the simulated time range translates to a share of 52.8% of the Nordic power system dimensioning fault, i.e. 1.4 GW [22]. A maximum of 82% of a turbine's kinetic energy can be utilized, while the 0.1 p.u. inertial power support allows an utilization of up to 23%.

Even though some of the above numerical results are specific to the Swedish system, the approach of analysis is generally applicable, and the conclusions can serve as a good reference for analyzing other power systems with converter-dominated generation systems. Future work should deal with the change in losses during the inertial support, the aggregation of alternative inertial support approaches such as the strategy

identified in [19], a comparison with inertial support from synchronous generation and the dynamic behaviour of the power system during frequency excursions with inertial support from wind turbines, respecting the findings of this work.

APPENDIX

WIND TURBINE MODEL PARAMETERS

$$\rho_{\text{air}} = 1.229 \text{ kg/m}^3, P_n = 3.6 \text{ MW}, R = 52 \text{ m}, \\ A_r = 2.3597 \times 10^{-3} \text{ m}^2/\text{W}, K_b = 62.337 \text{ m/s}$$

REFERENCES

- [1] EWEA, "Wind in power: 2017 european statistics," Feb. 2018.
- [2] P. Tielens and D. Van Hertem, "The relevance of inertia in power systems," *Renewable and Sustainable Energy Reviews*, vol. 55, pp. 999–1009, Mar. 2016.
- [3] G. Lalor, A. Mullane, and M. O'Malley, "Frequency control and wind turbine technologies," *IEEE Transactions on Power Systems*, vol. 20, no. 4, pp. 1905–1913, Nov. 2005.
- [4] R. Doherty, A. Mullane, G. Nolan, D. Burke, A. Bryson, and M. O'Malley, "An assessment of the impact of wind generation on system frequency control," *IEEE Transactions on Power Systems*, vol. 25, no. 1, pp. 452–460, Feb. 2010.
- [5] J. Ekanayake and N. Jenkins, "Comparison of the response of doubly fed and fixed-speed induction generator wind turbines to changes in network frequency," *IEEE Transactions on Energy Conversion*, vol. 19, no. 4, pp. 800–802, Dec. 2004.
- [6] N. Ullah, T. Thiringer, and D. Karlsson, "Temporary primary frequency control support by variable speed wind turbines - potential and applications," *IEEE Transactions on Power Systems*, vol. 23, no. 2, pp. 601–612, May 2008.
- [7] E. Muljadi, V. Gevorgian, M. Singh, and S. Santoso, "Understanding inertial and frequency response of wind power plants," IEEE, 2012.
- [8] F. Hafiz and A. Abdenour, "Optimal use of kinetic energy for the inertial support from variable speed wind turbines," *Renewable Energy*, vol. 80, pp. 629–643, 2015.
- [9] F. M. Gonzalez-Longatt, "Effects of the synthetic inertia from wind power on the total system inertia: Simulation study," IEEE, 2012.
- [10] R. Leelaruij and M. Bollen, "Synthetic inertia to improve frequency stability and how often it is needed," Energiforsk, 2015.
- [11] N. Miller, K. Clark, and M. Shao, "Impact of frequency responsive wind plant controls on grid performance," 2010.
- [12] L. Ruttledge, N. W. Miller, J. O'Sullivan, and D. Flynn, "Frequency response of power systems with variable speed wind turbines," *IEEE Transactions on Sustainable Energy*, vol. 3, no. 4, pp. 683–691, 2012.
- [13] B. G. Rawn, M. Gibescu, and W. L. Kling, "A static analysis method to determine the availability of kinetic energy from wind turbines," in *Power and Energy Society General Meeting*, IEEE, 2010, pp. 1–8.
- [14] L. Wu and D. Infield, "Power system frequency management challenges – a new approach to assessing the potential of wind capacity to aid system frequency stability," *IET Renewable Power Generation*, vol. 8, no. 7, pp. 733–739, 2014.
- [15] Goddard Earth Sciences Data and Information Services Center. (Jun. 11, 2016). MDISC data subset. [Online]. Available: <http://disc.sci.gsfc.nasa.gov/daac-bin/FTPSubset2.pl> (visited on 06/11/2016).
- [16] P. Jung, "System-wide evaluation of inertia support potentials from wind farms," Institutionen för energi och miljö, Elteknik, Chalmers tekniska högskola, 2017.
- [17] K. Clark, N. W. Miller, and J. J. Sanchez-Gasca, "Modeling of GE wind turbine-generators for grid studies," 2010.
- [18] J. Olauson, H. Bergström, and M. Bergkvist, "Scenarios and time series of future wind power production in sweden," Energiforsk, 2015.
- [19] M. Persson, "Frequency response by wind farms in power systems with high wind power penetration," PhD thesis, Chalmers University of Technology, Göteborg, 2017.
- [20] J. Brisebois and N. Aubut, "Wind farm inertia emulation to fulfill hydro-québec's specific need," in *Power and Energy Society General Meeting, 2011 IEEE*, IEEE, 2011, pp. 1–7.
- [21] M. Persson and P. Chen, "Frequency evaluation of the nordic power system using PMU measurements," (*Accepted for publication*), *IET Generation, Transmission & Distribution*, 2017.
- [22] ENTSO-E, "System operation agreement appendices," Sep. 20, 2017.